ORGANIC GEOCHEMICAL CHARACTERISTICS OF THE BILONG CO OIL SHALE (CHINA): IMPLICATIONS FOR PALEOENVIRONMENT AND PETROLEUM PROSPECTS

YUHONG ZENG[a], XIUGEN FU[a]*, SHENGQIANG ZENG[a,b], GU DU[a], JIANG CHEN[a], QIAN ZHANG[a], YIRONG ZHANG[a], YANLING YAO[a]

[a] Chengdu Institute of Geology and Mineral Resources, Chengdu 610081, China
[b] Chinese Academy of Geological Sciences, Beijing 100037, China

The Bilong Co oil shale is located in the southern part of the Qiangtang basin. This oil shale zone, together with the Shengli River-Changshe Mountain oil shale zone in the northern part of the Qiangtang basin, represents a large marine oil shale resource in China. An organic geochemical investigation of the oil shale was performed to reconstruct paleoenvironment during deposition and to assess petroleum prospects. The TOC content (6.75–19.2 wt.%) and S_2 values (5.96–70.2 mg HC/g rock) of oil shale samples from the Bilong Co area are relatively high indicating that the oil shale from the Bilong Co area has shale oil producing potential. The thermal maturity assessed from T_{max} and other maturity-related parameters (Ts/(Ts+Tm), C_{32}Hop S/(S+R), C_{29}St S/(S+R), and C_{29}St ββ/(αα+ββ)) shows a mature stage of the organic matter. Analyzed oil shale samples from the Bilong Co area are characterized by a dominance of low carbon number molecular compositions with relatively high C^{21-}/C^{21+} (0.82–1.95), low Pr/Ph (0.13–0.80), high concentrations of homo-hopanes (C_{31}-C_{35}), and a slight predominance of C_{29} steranes, indicating reducing environments, highly saline conditions, a strong contribution of inferior aquatic organisms, and some influence of terrestrial organic matter. Highly similar biomarker characteristics between the Bilong Co oil shale and nearby Zharen-Longeni crude oil in the southern Qiangtang depression suggest that the oil shale from the Bilong Co area has made a strong contribution to the generation of Zharen-Longeni crude oil.

Introduction

A rapid increase in consumption of energy and chemicals leads to a dramatic increase in the prices of conventional fossil resources [1] and stimulates the

---

* Corresponding author: e-mail *fuxiugen@126.com*

search for alternative energy. Oil shale, as an alternative energy source, has received much attention [2–4]. In China, oil shale deposits are widespread in many regions and were formed mainly in lacustrine environments, just like Tertiary oil shale in the Maoming, Huadian and Fushun areas [4], and Cretaceous oil shale in the Songliao and Minhe basins [5]. Marine oil shale was mainly found in the Qiangtang basin, northern Tibet, China, including the Bilong Co oil shale zone [6–8] and the Shengli River-Changshe Mountain oil shale zone [9–12]. These zones represent a large marine oil shale resource in China.

The Bilong Co oil shale is located in the southern part of the Qiangtang basin (Fig. 1a). Proved reserves are about 90.6 million tonnes [4]. The early studies of the oil shale were focused on the geochemistry of rare earth and trace elements [7–8] and anoxic event [13–14]. However, the data regarding the organic geochemistry of the oil shale from the Bilong Co area are still scarce and incomplete.

In the present study, we have investigated the organic geochemical characteristics of oil shale samples collected from the Bilong Co oil shale area. The primary aim was to reconstruct paleoenvironment during deposition and assess petroleum prospects.

Geological setting

From north to south, the Tibetan plateau is comprised of the Kunlun-Qaidam, Songpan-Ganzi flysch complex, Qiangtang, and Lhasa terranes, which are separated by the east-west trending Anyimaqen-Kunlun-Muztagh, Hoh Xil-Jinsha River and Bangong Lake-Nujiang River suture zones, respectively [8] (Fig. 1a). It is generally accepted that the paleo-Tethys represented by the present Jinsha River suture opened probably in the Early Carboniferous [15] and closed by the Permian to the latest Triassic [16]. The mid-Tethys branch between the Lhasa and Qiangtang terranes was open by the Early Jurassic [16] and closed along the Bangong Lake-Nujiang River suture during the Late Jurassic time [15].

The Qiangtang block, bounded by the Hoh Xil-Jinsha River suture zone to the north and the Bangong Lake-Nujiang River suture zone to the south, respectively, consists of the North Qiangtang depression, the South Qiangtang depression and the central uplift (Fig. 1b). The Bilong Co area is located in the South Qiangtang depression (Fig. 1b), where Jurassic marine deposits are widely spread including Lower Jurassic Quse Formation, Middle Jurassic Sewa Formation, Buqu Formation and Xiali Formation, and Upper Jurassic Suowa Formation (Fig. 1c). The Bilong Co oil shale zone is exposed for a distance of more than 4 km in an east-west trend. Abundant ammonites (*Harpoceras* sp.), occurring at the top of the Bilong Co oil shale section [13], indicate that the Bilong Co oil shale is of Early Jurassic age (i.e. Quse Formation strata).
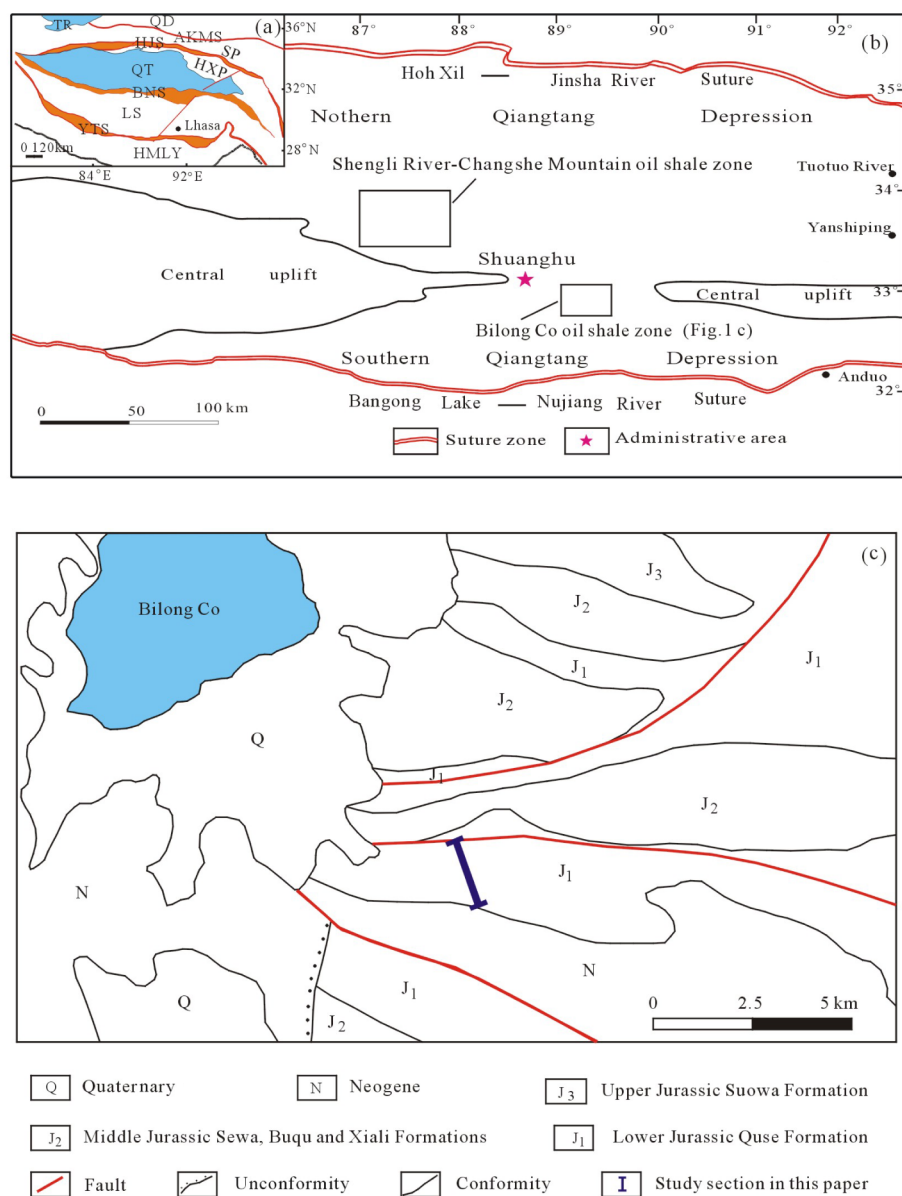
Fig. 1. (a) Map of the Tibetan plateau showing major Terranes. (b) Generalized map, showing location of the study area. (c) Simplified geological map of the Bilong Co area, showing location of oil shale section. TR, Tarim basin; QD, Qaidam; AKMS, Anyimaqen-Kunlun-Muztagh suture; HJS, Hoh Xil-Jinsha River suture; SP = Songpan-Ganzi flysch complex; HXP, Hoh Xili piedmont zone; QT, Qiagtang basin; BNS, Bangong Lake-Nujiang River suture; LS, Lhasa terrane; YTS, Yarlung Tsangpo suture; HMLY, Himalayas.

Samples and analytical methods

The investigated section is located in the Bilong Co area, South Qiangtang depression (Fig. 1b). A total of 18 samples were collected from the section. Thirteen of them were collected from oil shale seams with a vertical sampling interval of 1 m on average, and the other five samples were collected from micritic limestone layers. The present-day burial depth of the samples is about 50 cm.

The samples for geochemical analysis and Rock-Eval pyrolysis were all crushed and ground to 120 mesh. Total organic carbon (TOC) and Rock-Eval pyrolysis were determined using a TOC module-equipped Rock-Eval II type instrument. About 100 mg of sample was heated from ambient temperature up to 600 °C in a helium atmosphere [17]. These analyses were performed at the Geological Laboratory of Exploration and Development Research Institute of PetroChina Southwest Oil and Gasfield Company.

Analyzed samples were extracted with chloroform in a Soxhlet apparatus for 72 h. Extracts were separated into saturated hydrocarbons, aromatic hydrocarbons and polar NSO fractions by column chromatography using a silica gel-alumina column after the precipitation of asphaltenes [17]. Saturated fractions were analyzed by gas chromatography (GC) and gas chromatography-mass spectrometry (GC-MS). An aliquot of each saturated fraction was separated into *n*-alkanes and branched/cyclic alkanes by urea adduction.

The GC-MS analysis was performed using a Finnigan Voyager gas chromatography/mass spectrometer. This instrument was equipped with a DB5-MS fused silica capillary column of 30-m length, 0.25-μm film thickness and 0.32-mm inner diameter. Helium was used as the carrier gas. For routine GC analysis, the oven was isothermally held for 1 min at 35 °C, programmed from 35 to 120 °C at 10 °C/min, then from 120 to 300 °C at 3 °C/min, with a final holding time of 30 min [18]. The MS was operated with an ionization energy of 70 eV and a source temperature of 200 °C [18]. For the analysis of biomarkers, metastable ion transition for sterans (m/z 217) and triterpanes (m/z 191) was recorded at a dwell time of 25 ms per ion and a cycle time of 1 s. In order to identify the possible organic contaminations during the experimental processes, we added a blank sample for reference and no organic contamination discussed in this study was observed.

Results and discussion

Total organic carbon (TOC)

The TOC content of oil shale and micritic limestone samples from the Bilong Co area can be found in Table 1. The measurements exhibit that sediments in the study area as a whole are rich in organic matter with an average TOC of 7.38 wt.%. The TOC values of oil shale samples vary from

6.75–19.2 wt.% with an average of 9.70 wt.%, whilst the micritic limestone samples have relatively low TOC values ranging from 0.36–2.10 wt.% with an average of 1.35 wt.%.

Table 1. **Results of Rock-Eval/TOC analysis and calculated parameters**

Samples	Lithology	TOC[a]	S_1[b]	S_2[c]	S_3[d]	Kerogen type[e]	HI[f]	OI[g]	T_{max}[h]
BP-6	Micritic limestone	1.67	0.5	19.1	1.77	10.79	286.36	26.54	434
BP-7-1	Oil shale	6.75	0.51	20.16	1.7	11.86	298.67	25.19	437
BP-7-2	Oil shale	7.23	0.55	22.25	1.78	12.50	307.75	24.62	439
BP-7-3	Oil shale	6.91	0.5	20.67	1.68	12.30	299.13	24.31	432
BP-8	Micritic limestone	1.36	0.54	23.08	2.26	10.21	276.08	27.03	428
BP-9	Micritic limestone	0.36	0.03	0.3	1.16	0.26	83.33	322.22	443
BP-10-1	Oil shale	19.20	2.62	70.2	3.56	19.72	365.63	18.54	442
BP-10-2	Oil shale	7.95	0.4	5.96	0.93	6.41	202.03	31.53	434
BP-10-3	Oil shale	7.66	1.54	22.38	1.42	15.76	292.17	18.54	441
BP-10-4	Oil shale	9.11	1.26	23.79	1.83	13.00	261.14	20.09	441
BP-11	Micritic limestone	2.10	0.24	5.46	0.64	8.53	260.00	30.48	443
BP-12-1	Oil shale	10.27	1.3	30.19	2.64	11.44	293.96	25.71	441
BP-12-2	Oil shale	10.66	1.23	30.36	2.86	10.62	284.80	26.83	435
BP-12-3	Oil shale	7.13	0.47	14.91	2.28	6.54	209.12	31.98	442
BP-13	Micritic limestone	1.24	0.13	1.87	1.12	1.67	150.81	90.32	441
BP-14-1	Oil shale	10.96	1.25	36.48	2.78	13.12	332.85	25.36	442
BP-14-2	Oil shale	8.80	0.65	24.64	3.07	8.03	280.00	34.89	434
BP-14-3	Oil shale	13.50	1.2	39.98	3.55	11.26	296.15	26.30	439

[a] TOC (wt.%): total organic carbon content; [b] S_1 (mg HC/g rock): free hydrocarbons; [c] S_2 (mg HC/g rock): pyrolysable hydrocarbons; [d] S_3 (mg HC/g rock): carbon dioxide; [e]Kerogen type (S_2/S_3); [f] HI (mg HC/g TOC): hydrogen index; [g] OI (mg CO_2/g TOC):oxygen index; [h]T_{max} (°C): temperature of maximum S_2.

Rock-Eval pyrolysis

S_2 values of the studied samples vary from 0.3–70.2 mg HC/g rock (Table 1). S_2 values of 5.96–70.2 mg HC/g rock (Table 1) clearly indicate that oil shale samples from the Bilong Co area possess shale oil producing potential.

HI values of oil shale samples varying from 202.03–365.63 mg HC/g TOC indicate that the potential of these sediments is to produce the mixture of oil and gas, which is in agreement with the kerogen-type index (S_2/S_3 ratios) (Table 1). According to the HI vs. OI diagram [19] (Fig. 2), analyzed samples can be classified as mostly type II kerogen. The T_{max} values of most samples, between 435 and 443 °C (Table 1), indicate that the organic matter is thermally mature.
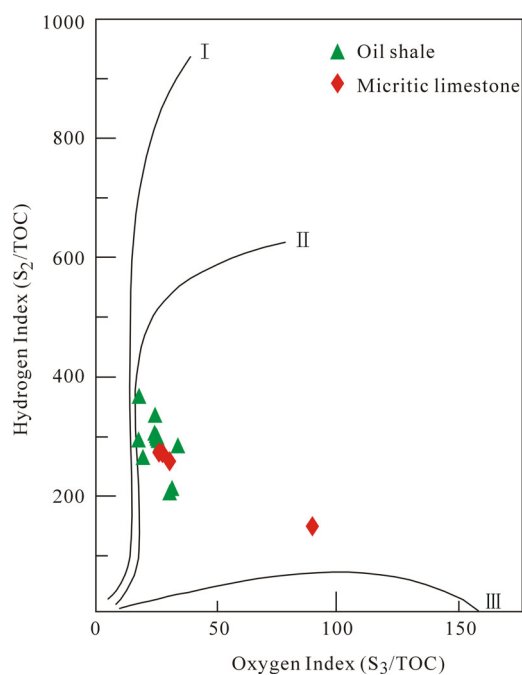
Fig. 2. Plot of hydrogen index versus oxygen index for the analyzed samples from the Bilong Co oil shale area.

Molecular composition of the organic matter

Normal alkanes and isoprenoid hydrocarbons

Partial gas chromatograms of the saturated hydrocarbons extracted from the sediments of Bilong Co samples are shown in Fig. 3 and their parameters are listed in Table 2. The normal alkanes (*n*-alkanes) are represented by C_{14-35} homologues and the distributions through the sections are very similar. The GC traces of all samples studied demonstrate a unimodal distribution typically dominated by components of lower molecular weight (the C_{21}^-/C_{21}^+ ratios of most samples are from 1.06 to 1.95, Table 2), with a distribution maximum among the lighter hydrocarbons (C_{17}-C_{19}) and without a distinct odd or even predominance (the OEP values ranging from 0.88-1.07, Table 2), except the sample BP-9. The *n*-alkane distribution of the sample BP-9 is dominated by mid-chain *n*-alkanes with a marked even over odd predominance in the C_{22}-C_{28} region and without a clearly unimodal or bimodal distribution (Fig. 3).

The isoprenoid hydrocarbons pristane (Pr) and phytane (Ph) are identified in all of the samples taken from the Bilong Co area. The analyzed samples exhibit lower values of Pr/Ph ratios, varying from 0.13 to 0.88. Most of oil shale samples have the Pr/Ph ratios <0.6 (Table 2). The Pr/n-C_{17} and Ph/n-C_{18} ratios are listed in Table 2, and a plot of Pr/n-C_{17} vs. Ph/n-C_{18} [20] is shown in Fig. 4.
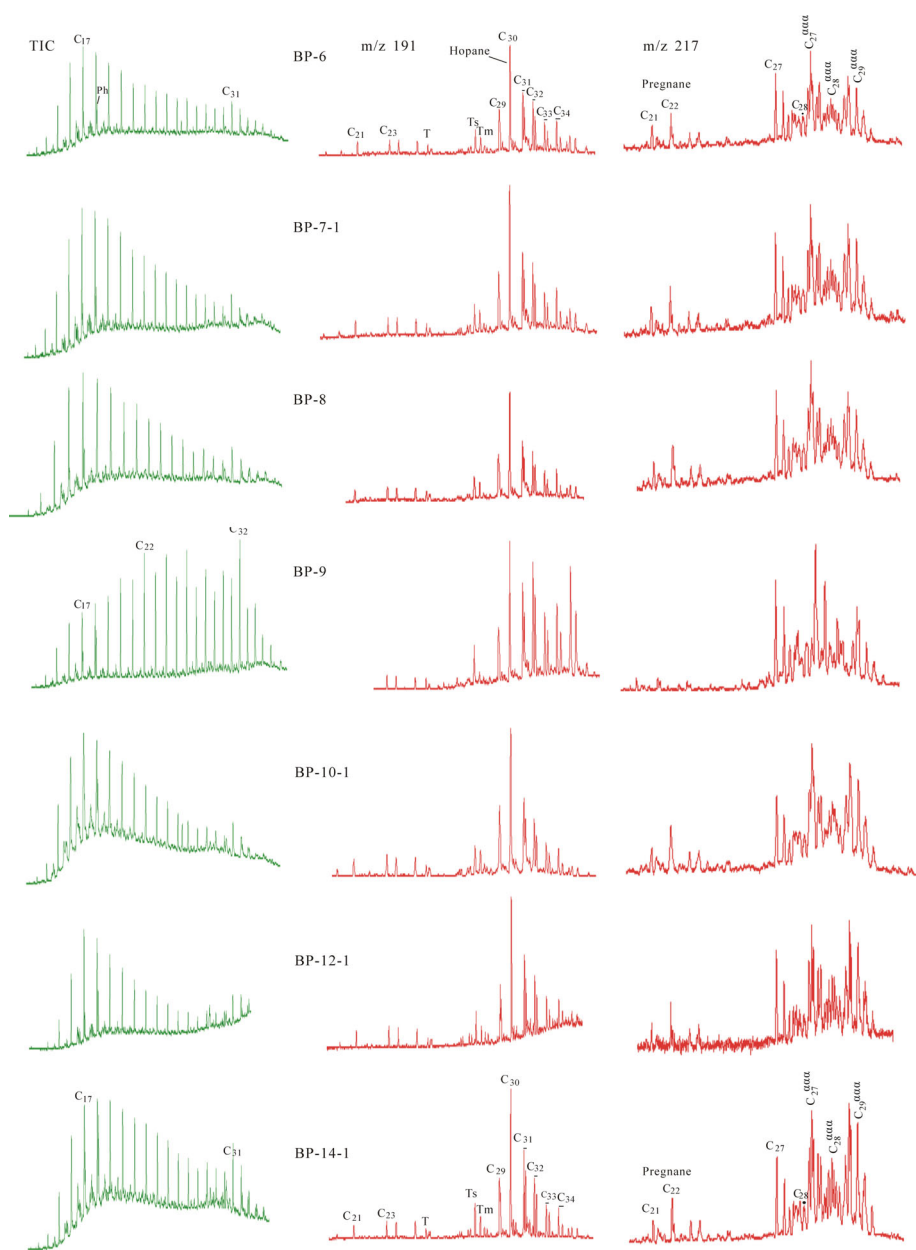
Fig. 3. TIC, terpane and sterane mass chromatograms of samples from the Bilong Co oil shale area.

Table 2. **Biomarker parameters calculated based on m/z 191 and m/z 217 mass chromatograms**

Samples	Lithology	Parameters of normal alkanes and isoprenoid hydrocarbons					Parameters of terpanes				Parameters of steranes				
		A	B	C	D	E	F	G	H	I	J	K	% C$_{27}$	% C$_{28}$	% C$_{29}$
BP-6	M. l*	1.15	0.98	0.88	0.23	0.32	0.60	0.58	0.11	1.55	0.40	0.46	46	17	37
BP-7-1	Oil shale	1.38	0.99	0.70	0.19	0.31	0.55	0.58	0.07	1.57	0.50	0.42	38	22	40
BP-7-2	Oil shale	1.33	0.88	0.80	0.24	0.33	0.54	0.59	0.10	1.56	0.50	0.41	40	24	36
BP-7-3	Oil shale	1.61	0.93	0.71	0.19	0.27	0.53	0.55	0.15	1.51	0.44	0.41	42	16	43
BP-8	M. l*	1.06	0.90	0.83	0.23	0.30	0.58	0.58	0.26	1.59	0.48	0.44	39	23	39
BP-9	M. l*	0.29	0.81	0.49	0.32	0.59	0.60	0.61	0.40	1.58	0.49	0.54	37	27	35
BP-10-1	Oil shale	1.95	0.95	0.44	0.17	0.43	0.56	0.59	0.12	1.83	0.49	0.43	38	21	41
BP-10-2	Oil shale	0.82	0.95	0.49	0.33	0.79	0.67	0.60	0.09	1.50	0.46	0.46	36	20	45
BP-10-3	Oil shale	1.20	0.94	0.41	0.26	0.75	0.67	0.58	0.11	2.28	0.47	0.46	35	21	44
BP-10-4	Oil shale	1.79	1.03	0.37	0.28	0.87	0.67	0.58	0.09	1.96	0.38	0.52	36	21	43
BP-11	M. l*	1.30	0.98	0.40	0.19	0.43	0.67	0.56	0.09	1.74	0.23	0.51	39	27	34
BP-12-1	Oil shale	1.56	1.03	0.35	0.19	0.54	0.64	0.59	0.10	1.61	0.46	0.46	35	21	44
BP-12-2	Oil shale	1.62	0.98	0.40	0.20	0.53	0.65	0.56	0.08	1.95	0.39	0.50	34	23	43
BP-12-3	Oil shale	1.22	0.97	0.47	0.25	0.55	0.64	0.56	0.07	1.69	0.42	0.43	34	19	47
BP-13	M. l*	0.91	0.97	0.34	0.30	0.97	0.66	0.56	3.11	2.14	0.38	0.53	33	25	41
BP-14-1	Oil shale	1.37	0.98	0.46	0.29	0.70	0.63	0.56	0.08	1.65	0.38	0.48	35	20	45
BP-14-2	Oil shale	0.87	0.98	0.13	0.20	0.48	0.62	0.56	0.08	1.78	0.35	0.48	35	20	45
BP-14-3	Oil shale	1.31	1.07	0.20	0.19	0.48	0.63	0.57	0.08	1.65	0.37	0.50	37	21	42

A: C_{21}^{-}/C_{21}^{+}; B: OEP; C: Pr/Ph (pristane/phytane); D: Pr/nC$_{17}$ (pristane/normal-C$_{17}$); E: Ph/nC$_{18}$ (phytane /normal-C$_{18}$); F: Ts/(Ts+Tm) (Ts: 18α(H), 22, 29, 30-trisnorneohopane; Tm: 17α(H), 22, 29, 30-trisnorhopane); G: C$_{32}$Hop 22S/(22S+22R) (17α(H), 21β(H)-bis-homohopane (22S)/[17α(H), 21β(H)-bishomohopane (22S)+ 17α(H), 21β(H)-bishomohopane (22R)] of C$_{32}$ homohopane); H: G index (gammacerane/C$_{30}$ hopane); I: C$_{25}$ tri/C$_{26}$ tri (C$_{25}$ tricyclic terpanes/C$_{26}$ tricyclic terpanes); J: C$_{29}$St 20S/(20S+20R) (5α(H), 14α(H), 17α(H)-20S/[5α(H), 14α(H), 17α(H)-20S+5α(H), 14α(H), 17α(H)-20R] of C$_{29}$ sterane); K: C$_{29}$St ββ/(αα+ββ) (C29-regular sterane (20αββR+20αββS)/(20αααS+20αααR+20αββR+20αββS) isomer ratio.
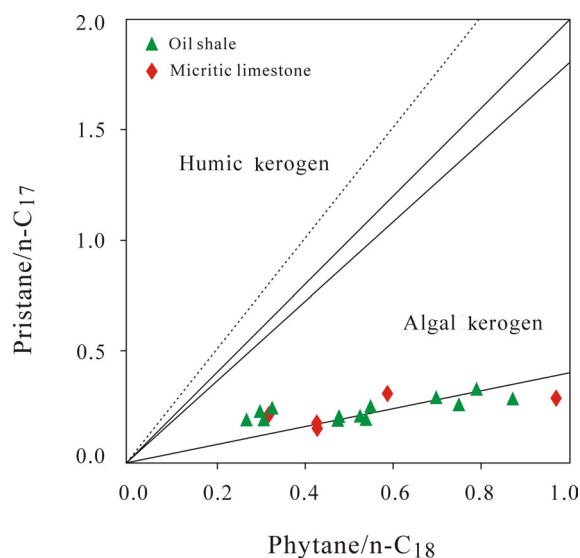
M. l* – micritic limestone.

Fig. 4. Plot of Pr/nC$_{17}$ and Ph/nC$_{18}$ alkane ratios [20] for oil shale and micritic limestone samples from the Bilong Co area.

Terpanes

The distributions and relative abundances of tricyclic, tetracyclic and pentacyclic terpanes obtained from m/z 191 ion chromatograms are given in Fig. 3 and their parameters are summarized in Table 2. Tricyclic terpanes exhibit low concentrations in all samples from the Bilong Co area ranging from C_{19} to C_{29}, and dominated by low molecular weight compounds (C_{20}-C_{25}) with a maximum at C_{25}. The traces of m/z 191 ion chromatograms show dominant pentacyclic triterpenoids in the C_{29}-C_{35} range maximizing at C_{30} hopane in all oil shale samples. Gammacerane was recorded in low amounts for all samples, with a gammacerane index (gammacerane/C_{30} hopane) varying from 0.07-3.11. The component 18α(H)-trisnorneohopane (Ts) is dominant over its counterpart 17α(H)-trisnorhopane (Tm), with a Ts/(Ts+Tm) ratio ranging from 0.53 to 0.67 in all samples analyzed. The C_{31} hopane and higher homologues occur as 22S and 22R epimers. The 22S/(22S+22R) ratios for C_{32} hopane in all samples studied vary from 0.55–0.61 with a mean value of 0.58.

Steranes

The m/z 217 mass chromatograms recorded the sterane distributions of samples analyzed in Fig. 3, and the correlative parameters of steranes are listed in Table 2. Some samples exhibit a slight predominance of C_{29} sterane (samples BP-7-1, BP-7-3, BP-10-1, BP-10-2, BP-10-3, BP-10-4, BP-12-1, BP-12-2, BP-12-3, BP-13, BP-14-1, BP-14-2, BP-14-3). As for the samples BP-6, BP-7-2, BP-9 and BP-11, C_{27} is observed as a dominant sterane. Steranes of the BP-8 micritic limestone show a V-shaped pattern (Fig. 3),

namely $C_{27} > C_{28} < C_{29}$, as well as $C_{27} = C_{29}$. The steranes/hopanes (St/Hop) ratios show low values for all samples varying from 0.16 to 0.38.

Type/source of organic matter

The distributions of *n*-alkanes can be used to indicate the source of organic matter [21]. Saturated hydrocarbons of most samples exhibit a dominance of low molecular weight components with the highest peaks at *n*-C_{17}, C_{18}, or C_{19} (Fig. 3). The predominance of lighter hydrocarbons in most oil shale samples (the C_{21}^{-}/C_{21}^{+} ratios are from 0.82 to 1.95 with an average of 1.39, Table 2) can be an indicator of algal organic matter [22] or/and bacterial biomass input [23]. In contrast, *n*-alkanes from the micritic limestones show a different distribution. The C_{21}^{-}/C_{21}^{+} ratios for the samples BP-6, BP-8, BP-9, BP-11, and BP-13 are 1.15, 1.06, 0.29, 1.30, and 0.91, respectively. The distribution of *n*-alkanes in the sample BP-9 shows a dominance of mid-chain *n*-alkanes with a distinct even (nC$_{22, 24, 26, 28}$)-over-(nC$_{21, 23, 25, 27}$)-odd predominance (Fig. 3). Even over odd distribution in *n*-alkanes is usually considered a common feature for organic matter deposited in saline environments [22]. Generally, these *n*-alkanes with an even over odd distribution can directly originate from bacterial lipids [24] or be produced by a secondary process involving thermal decomposition of lipid precursors (e.g., *n*-fatty acids) [25]. Considering the geochemical parameters for the depositional environments (e.g., Pr/Ph ratios, Table 2) and carbonate contents of strata, the *n*-alkane distribution patterns in our case are believed to be independent of the redox conditions and the mineral composition of strata, but to be associated with the composition of original organic matter [26]. Hence, a strong even predominance within mid-chain-length *n*-alkanes in our study may be ascribed to a contribution of halophilic bacteria or/and microorganisms from deep saline environments to organic matter accumulation [26].

Pr/*n*-C_{17} and Ph/*n*-C_{18} ratios are usually associated with source rock types, depositional environments and organic matter maturity [23]. A plot of Pr/*n*-C_{17} vs. Ph/*n*-C_{18} is shown in Fig. 4. Clearly, most of samples from the Bilong Co area, whether oil shale or micritic limestone samples, plot in the region designated for algal kerogens, suggesting that these rock extracts contain considerable amounts of algal organic matter.

The distribution of regular steranes has been applied to determine the organic matter source of crude oils [27]. Huang and Meinshein [28] found that a predominance of C_{29} sterols would reflect a contribution of higher plants to organic matter accumulation, whereas a dominance of C_{27} homologues would be an indicator of marine plankton. Based on their work, the relative abundances of steranes are used to infer biological source of organic matter in oils [27]. However, this approach must be used with caution in interpreting C_{29} sterane predominances. Volkman [29] found that some marine sediments, including those deposited in pelagic environments far from terrigenous influence, showed a predominance of C_{29} steranes, and thus concluded that there must be unproven marine source of the C_{29} steranes.

The relative abundances of C_{27}, C_{28}, and C_{29} regular steranes in oil shale samples are in the range of 34–42%, 16–24%, and 36–47%, respectively (Table 2). Although most oil shale samples show slight higher C_{29} regular sterane contents compared to C_{27} and C_{28} regular steranes, obviously, their relative amounts of C_{27} regular steranes are close to C_{29} homologues. Combined with other biomarker parameters (e.g., *n*-alkane distribution; Pr/n-C_{17} vs. Ph/n-C_{18} diagram), a slight predominance of C_{29} steranes in oil samples probably reflects a strong contribution of inferior aquatic organisms (e.g., algae; bacteria; microorganisms), and some influence of terrestrial organic matter. In contrast, micritic limestone samples exhibit a different distribution; their regular sterane content generally shows a predominance of C_{27} steranes, indicating a contribution of aquatic algae or/and microbial activity. In addition, steranes of the BP-8 micritic limestone show a V-shaped pattern (Fig. 3), namely $C_{27}>C_{28}<C_{29}$ as well as $C_{27}=C_{29}$, also revealing mixed contributions from bacterial and higher plant wax sources.

Thermal maturity of organic matter

Thermal maturity of organic matter in sediments is determined by the creation process of hydrocarbons through undergoing a series of physical or/and chemical changes by different agents such as heat, pressure, burial and time after deposition. Maturity-related parameters including T_{max}, Ts/(Ts+Tm) ratio, the 22S/(22S+22R) ratio for C_{32} homohopane and the 20S/(20S+20R) and $\beta\beta/(\alpha\alpha+\beta\beta)$ ratios for C_{29} sterane are used as the possible indicators for organic maturity in our work. The T_{max} values of most samples, between 435 °C and 443 °C (Table 1), indicate that the organic matter in sediments is thermally mature. The Ts/(Ts+Tm) ratio increases from nearly 0 to close to 1 with increasing maturity. The equilibrium value for Ts/(Ts+Tm) ratio is measured to be 0.52–0.55 [30]. Analyzed samples show high Ts/(Ts+Tm) ratios with an average of 0.62 (i.e., in the range of 0.53–0.67 & 0.58–0.67 for the extracts of oil shale and micritic limestone samples respectively, Table 2), indicating the mature characteristics of oil shale and micritic limestone samples in the Bilong Co area. The 22S/(22S+22R) extended hopane ratio increases with increasing maturity and has been widely used as a maturity indicator [23]. The 22S/(22S+22R) homohopane ratios for C_{32} hopane varying from 0.55 to 0.61 with an average of 0.58 are close to equilibrium values (0.57-0.62) indicating that the organic matter is thermally mature. The 20S/(20S+20R) together with $\beta\beta/(\alpha\alpha+\beta\beta)$ isomerization ratios of the C_{29} steranes are usually used as indicators of maturity. In the Bilong Co area, analyzed samples exhibit the 20S/(20S+20R) sterane ratios varying from 0.23 to 0.50, whereas, the ratios of $\beta\beta/(\alpha\alpha+\beta\beta)$ are in the range of 0.41 to 0.54. According to the C_{29}St 20S/(20S+20R) vs. C_{29}St $\beta\beta/(\alpha\alpha+\beta\beta)$ diagram (Fig. 5) [31], most of samples are plotted in the mature area, indicating the mature characteristics of the organic matter in sediments, thus supporting other indicators for organic maturity as mentioned above.
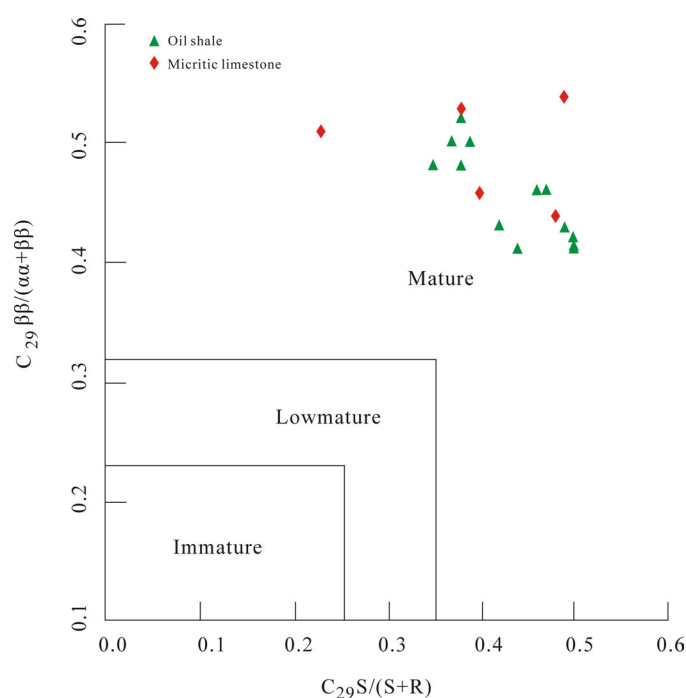
Fig. 5. The maturation of oil shale and micritic limestone samples based on sterane parameters.

Depositional environment

Pr/Ph ratio, an indicator of redox potential of source sediments proposed by Didyk et al. [32], has been widely utilized in many studies to infer oxicity or anoxicity of depositional environments and source of organic matter. High Pr/Ph ratios (>3) are usually associated with suboxic to oxic depositional environments, however, low Pr/Ph ratios (<0.6) indicate anoxic depositional conditions and usually hypersaline envirnments [23]. As seen in Table 2, analyzed samples show low Pr/Ph ratios (<1) and the Pr/Ph values of most samples are <0.6. The low values of Pr/Ph, combined with some pyrite crystals found in oil shale samples [7], indicate that oil shale and micritic limestone samples in the Bilong Co area were deposited in aquatic and probably saline environments under reducing bottom conditions.

Although the origin of tricyclic terpanes is controversial, they have been widely used as environment indicators [26]. The low concentrations of tricyclic terpanes in all samples from Bilong Co area indicate a marine environment organism precursor as the source of these biomarkers [12]. The C_{25}/C_{26} tricyclic terpane ratio has also been successfully applied as an environment parameter to distinguish the marine and non-marine depositional environments [33]. The values of C_{25}/C_{26} (>1) indicate a marine environment; however, the low C_{25}/C_{26} tricyclic terpane ratio is usually associated with a non-marine environment. The high values of C_{25}/C_{26} in

most samples from the Bilong Co area suggest that these rocks have been deposited in a marine environment (Table 2).

Gammacerane, a C_{30} triterpane first identified in bitumen of the Green River shale, is usually considered an indicator of hypersaline marine and nonmarine depositional environments [34]. Gammacerane index (GI: gammacerane/hopane) increases with increasing salinity of depositional conditions [23]. In this study, the gammacerane indices ranging from 0.07 to 0.15 in the oil shale samples, and from 0.09 to 3.11 in the micritic limestones (Table 2), probably suggest highly saline conditions, which can also be supported by the distribution pattern of even over odd dominance in mid-chain-length *n*-alkanes in the sample BP-9. GI, combined with other biomarker parameters (e.g., Pr/Ph ratio; C_{25}/C_{26} tricyclic terpane ratio) in our case probably indicate that analyzed samples from the Bilong Co area were deposited in a hypersaline marine environment under anoxic conditions.

Potential of hydrocarbon generation and oil-source rock correlation

The analytical data for oil shale samples from the Bilong Co area show that they possess hydrocarbon generation potential (Table 1) with greater than 6 wt.% of total organic carbon content and more than 27 mg HC/g rock of the average S_2 value, whereas the source-rock potential of micritic limestone samples is relatively low. The HI index values of oil shale samples are in the range of 202.03–365.63 with the average of 286.42 (Table 1). As seen from Fig. 2, obviously, all oil shale samples are plotted more close to the oil-forming curve. These HI values indicate that oil shale samples from the Bilong Co area possess more oil-prone potential than gas-prone potential. This interpretation is consistent with the high S_2/S_3 rates of oil shale samples (6.41–19.72). The rate of S_2/S_3 higher than 5 also indicates that these oil shale samples can generate oil.

Correlation between the characteristics of the oil shale in Bilong Co area and those of their potential oils in this study was attempted using biomarker parameters based on the GC, GC-MS. The biomarker characteristics of the Bilong Co oil shale are very similar to that of Zharen-Longeni crude oil in the southern Qiangtang depression (Fig. 6), suggesting that the oil shale in the Bilong Co area has made a strong contribution to the generation of Zharen-Longeni crude oil. Wang et al. [35] also found the correlation between the Bilong Co oil shale and Longeni oils by using carbon isotope data and biomarker parameters. The carbon isotope curves of the Bilong Co oil shale and Longeni oils almost match and their homohopane indices and diasterane contents are highly similar, suggesting that the Longeni oils could have been sourced from the oil shale in Bilong Co area. The oil-source rock correlation between the Bilong Co oil shale and crude oil in the southern Qiangtang depression is also supported by the research of Fu et al. [36]. They inferred, based on the similar carbon isotope compositions in both oil shale and oils, that the Bilong Co oil shale could be one of the source rocks of Zharen crude oil in the southern Qiangtang depression.
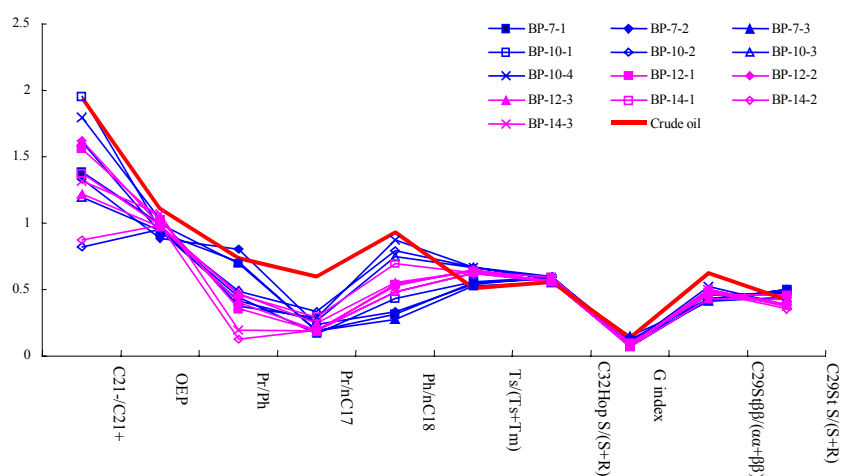
Fig. 6. Comparison of biomarkers between the Bilong Co oil shale and Zharen-Longeni crude oil in the southern Qiangtang depression.

Conclusions

1. The TOC content and S_2 values of oil shale samples from the Bilong Co area are high indicating that the oil shale from the Bilong Co area has shale oil producing potential. Thermal maturity assessed by T_{max} shows a mature stage of the organic matter.

2. The Bilong Co oil shale is characterized by a dominance of low carbon number molecular compositions with relatively high C^{21-}/C^{21+} (0.82–1.95), low Pr/Ph (0.13–0.80), high concentrations of homohopanes (C_{31}-C_{35}), and a slight predominance of C_{29} steranes, indicating reducing environments, highly saline conditions, a strong contribution of inferior aquatic organisms, and some influence of terrestrial organic matter.

3. The biomarker characteristics of the Bilong Co oil shale are very similar to that of oil seepages in the southern Qiangtang depression, suggesting that the oil shale in the Bilong Co area has made a strong contribution to the generation of these oils.

Acknowledgements

REFERENCES

1. *Cao, J. P., Zong, Z. M., Zhao, X. Y., Liu, G. F., Mou, J., Wang, F., Huang, Y. G., Zhou, G. J., Hu, H. Q., Wei. X. Y.* Chemical composition of carbon disulfide-extractable fraction from oil shales of three Chinese deposits // Oil Shale. 2007. Vol. 24, No. 3. P. 423–433.
2. *Dyni, J. R.* Oil shale developments in the United States // Oil Shale. 2006. Vol. 23, No. 2. P. 97–98.
3. *Kök, M. V.* Oil shale resources in Turkey // Oil Shale. 2006. Vol. 23, No. 3. P. 209–210.
4. *Liu, Z. J., Yang, H. L., Dong, Q. S., Zhu, J. W., Guo, W., Ye, S. Q., Liu, R., Meng, Q. T., Zhang, H. L., Gan, S. C.* Oil Shale in China. – Beijing: Petroleum Industry Press, 2009. P. 98–167 [in Chinese with English abstract].
5. *Qian, J. L., Yin, L., Wang, J. Q., Li, S. Y., Han, F., He, Y. G.* Oil Shale – a Complementary Energy of Petroleum. – Beijing: Sinopec Press, 2008. P. 14–23 [in Chinese].
6. *Wang, C. S., Zhang, S. M.* The discovery of oil shales in the Shuanghu area, northern Tibet, China // Geology in China. 1987. Vol. 8, No. 11. P. 29–31 [in Chinese].
7. *Fu, X. G., Wang, J., Zeng, Y. H., Tan, F. W., Chen, W. B., Feng, X. L.* Geochemistry of rare earth elements in marine oil shale – a case study from the Bilong Co area, northern Tibet, China // Oil Shale. 2010. Vol. 27, No. 3. P. 194–208.
8. *Fu, X. G., Wang, J., Zeng, Y. H., Tan, F. W., Feng, X. L.* Concentration and mode of occurrence of trace elements in marine oil shale from the Bilong Co area, northern Tibet, China // Int. J. Coal Geol. 2011. Vol. 85, No. 1. P. 112–122.
9. *Fu, X. G., Wang, J., Qu, W. J., Duan, T. Z., Du, A. D., Wang, Z. J., Liu, H.* Re-Os (ICP-MS) dating of marine oil shale in the Qiangtang basin, Northern Tibet, China // Oil Shale. 2008. Vol. 25, No. 1. P. 47–55.
10. *Fu, X. G., Wang, J., Zeng, Y. H., Tan, F. W., He, J. L.* Concentrations and modes of occurrence of platinum group elements in the Shengli River oil shale, northern Tibet, China // Fuel. 2010. Vol. 89, No. 12. P. 3623–3629.
11. *Fu, X. G., Wang, J., Tan, F. W., Zeng, Y. H.* Sedimentological investigations of the Shengli River-Changshe Mountain oil shale (China): relationships with oil shale formation // Oil Shale. 2009. Vol. 26, No. 3. P. 373–381.
12. *Fu, X. G., Wang, J., Zeng, Y. H., Tan, F. W., Feng, X. L.* REE geochemistry of marine oil shale from the Changshe Mountain area, northern Tibet, China // Int. J. Coal Geol. 2010. Vol. 81, No.3. P. 191–199.
13. *Yi, H. S., Deng, B., Xiong, S. P.* Lower Jurassic oil shale deposition from northern Tibet: chemostratigraphic signals and the early Toarcian anoxic event // 18th HKT Workshop Abstracts. 2003. P. 129–130.
14. *Chen, L., Yi, H. S., Hu, R. Z., Zhong, H., Zou, Y. R.* Organic geochemistry of the Early Jurassic oil shale from the Shuanghu area in Northern Tibet and the Early Toarcian oceanic anoxic event // Acta Geol. Sin. Engl. 2005. Vol. 79, No. 3. P. 392–397.
15. *Yin, A., Harrison, T. M.* Geologic evolution of the Himalayan-Tibetan Orogen // Annu. Rev. Earth Pl. Sci. 2000. Vol. 28. P. 211–280.

16. *Kapp, P., Yin, A., Manning, C. E., Harrison, T. M., Taylor, M. H., Ding, L.* Tectonic evolution of the early Mesozoic blueschist-bearing Qiangtang metamorphic belt, central Tibet // Tectonics. 2003. Vol. 22, No. 4. P. 1043.

17. *Fu, X. G., Wang, J., Zeng, Y. H., Li, Z. X., Wang, Z. J.* Geochemical and palynological investigation of the Shengli River marine oil shale (China): implications for paleoenvironment and paleoclimate // Int. J. Coal Geol. 2009. Vol. 78, No. 3. P. 217–224.

18. *Xiong, Y. Q., Geng, A. S.* Carbon isotopic composition of individual *n*-alkanes in asphaltene pyrolysates of biodegraded crude oils from the Liaohe Basin, China // Org. Geochem. 2000. Vol. 31, No. 12. P. 1441–1449.

19. *Espitalié, J., Laporte, J. L., Madec, M., Marquis, F., Leplat, P., Paulet, J., Boutefeu, A.* Méthode rapide de caractérisation des roches mères, de leur potentiel pétrolier et de leur degré d'évolution // Rev. I. Fr. Petrol. 1977. Vol. 32, No. 1. P. 23–42.

20. *Connan, J., Cassou, A. M.* Properties of gases and petroleum liquids derived from terrestrial kerogen at various maturation levels // Geochim. Cosmochim. Ac. 1980. Vol. 44, No. 1. P. 1–23.

21. *Volkman, J. K., Farrington, J. W., Gagosian, R. B., Wakeham, S. G.* Lipid composition of coastal marine sediments from the Peru upwelling region // Advance in Organic Geochemistry / Bjorøy M. et al. (eds.). – New York: Wiley, 1981. P. 228–240.

22. *Tissot, B. P., Pelet, R., Roucache, J., Combaz, A.* Alkanes as geochemical fossils indicators of geological environments // Advances in Organic Geochemistry / Campos, R., Goni, J. (Eds.). 1975. Enadimsa, Madrid. 1977. P. 117–154.

23. *Peters, K. E., Moldowan, J. M.* The Biomarker Guide: Interpreting Molecular Fossils in Petroleum and Ancient Sediments. – New Jersey: Prentice Hall, 1993. P. 483–664.

24. *Grimalt, J., Albaiges, J.* Sources and occurrence of C_{12}-C_{22} *n*-alkane distributions with even carbon-number preference in sedimentary environments // Geochim. Cosmochim. Ac. 1987. Vol. 51, No. 6. P. 1379–1384.

25. *Shimoyama, A., Johns, W. D.* Formation of alkanes from fatty acids in the presence of $CaCO_3$ // Geochim. Cosmochim. Ac. 1972. Vol. 36, No. 1. P. 87–91.

26. *Zhu, Y. M., Weng, H. X., Su, A. G., Liang, D. G., Peng, D. H.* Geochemical characteristics of Tertiary saline lacustrine oils in the Western Qaidam Basin, northwest China // Appl. Geochem. 2005. Vol. 20, No. 10. P. 1875–1889.

27. *Moldowan, J. M., Seifert, W. K., Gallegos, E. J.* Relationship between petroleum composition and depositional environment of petroleum source rocks // Am. Assoc. Petr. Geol. B. 1985. Vol. 69, No. 8. P. 1255–1268.

28. *Huang, W. Y., Meinschein, W. G.* Sterols as ecological indicators // Geochim. Cosmochim. Ac. 1979. Vol. 43, No. 5. P. 739–745.

29. *Volkman, J. K.* A review of sterol markers for marine and terrigenous organic matter // Org. Geochem. 1986. Vol. 9, No. 2. P. 83–99.

30. *Seifert, W. K., Moldowan, J. M.* Use of biological markers in petroleum exploration // Biological Markers in the Sedimentary Record / Johns, R. B. (ed.). – Amsterdam: Elsevier, 1986. P. 261–290.

31. *Chen, J. Y., Bi, Y. P., Zhang, J. G., Li, S. F.* Oil-source correlation in the Fulin basin, Shengli petroleum province, East China. // Org. Geochem. 1996. Vol. 24, No. 8-9. P. 931–940.

32. *Didyk, B. M., Simoneit, B. R. T., Brassell, S. C., Eglinton, G*. Organic geo-
     chemical indicators of paleoenvironmental conditions of sedimentation //
     Nature. 1978. Vol. 272. P. 216–222.

33. *Hanson, A. D., Zhang, S. C., Moldowan, J. M., Liang, D. G., Zhang, B. M*.
     Molecular organic geochemistry of the Tarim Basin, Northwest China // Am.
     Assoc. Petr. Geol. B. 2000. Vol. 84, No. 8. P. 1109–1128.

34. *ten Haven, H. L., de Leeuw, J. W., Sinninghe Damsté, J. Schenck, P. A.,
     Palmer, S. E., Zumberge, J*. Application of biological markers in the recognition
     of palaeo-hypersaline environments // Lacustrine Petroleum Source Rocks.
     Geological Society Special Publication / Fleet, A. J., Kelts, K., Talbot, M. R.
     (Eds.). Vol. 40. – Oxford, Blackwell, 1988. P. 123–130.

35. *Wang, C. S., Yi, H. S., Liu, C. Y., Li, Y. L., Zou, Y. R., Wu, X. H., Deng, B.,
     Yang, X. K*. Discovery of paleo-oil-reservoir in Qiangtang basin in Tibet and its
     geological significance // Oil & Gas Geology. 2004. Vol. 25, No. 2. P. 139–143
     [in Chinese with English abstract].

36. *Fu, X. G., Liao, Z. L., Wang, J., Chen, W. B*. Geochemistry and significance of
     oil seepages in the Zaring area of the Southern Qiangtang depression, nothern
     Tibet // Acta Sedimentologica Sinica. 2008. Vol. 26, No. 4. P. 697–703 [in
     Chinese with English abstract].